人工臓器

日本人工臓器学会
Vol.39 No.2 2010
ISSN 0300-0818
第39巻　第2号
平成22年11月1日発行
年3回発行

2

The Japanese Journal of Artificial Organs

第48回日本人工臓器学会大会予稿集

121　年齢別にみた大動脈弁置換術前後の左室収縮能、拡張能の検討
　　本田賢太朗　(和歌山県立医科大学　第一外科)
122　慢性透析患者における機械弁使用の妥当性の検討
　　堂前圭太郎　(国立循環器病研究センター)
123　感染性心内膜炎手術における人工物の使用と遠隔成績
　　桑原　史明　(名古屋大学大学院心臓外科)
124　人工心臓弁の機能不全発症に関わる遺伝子多型の探索のための SNP 解析
　　澤田　留美　(国立医薬品食品衛生研究所医療機器部)

〔一般演題〕 14:00 ～ 14:40

人工心臓 (6)

座長：　徳永　滋彦　(神奈川県立循環器呼吸器病センター)
　　田中　　明　(福島大学共生システム理工学類)
125　完全体内埋込型人工心臓駆動用経皮エネルギー伝送システム―空心型経皮トランスフォーマーのコイル寸法の検討―
　　若林　春貴　(東京理科大学大学院理工学研究科電気工学専攻)
126　生体組織電気特性を利用した体内 - 体外通信システムの通信特性と評価
　　加藤　良都　(東海大学大学院理工学研究科電子情報工学専攻)
127　光電子増倍管による微弱発光を観測するための経時的計測装置の開発
　　掛川　竜馬　(大阪工業大学大学院工学研究科生体医工学専攻)

〔教育講演２〕 14:40 ～ 15:10

座長：　阿部　裕輔　(東京大学大学院医学系研究科)

EL2　Intra-dialytic electrostimulation of leg extensors may improve physical fitness in hemodialysis patients
　　Petr Dobsak (St. Anna Faculty Hospital and Masaryk University of Brno, Czech Republic)

〔一般演題〕 15:10 ～ 16:25

環境・生理

座長：　花崎　和弘　(高知大学医学部　外科学講座外科 1)
　　柴田　宗一　(宮城県立循環器・呼吸器病センター)
128　ICU 患者における人工膵臓の血糖変動抑制に関する検討
　　矢田部智昭　(高知大学教育研究部医療学系医学部門麻酔科学講座)
129　ラット末梢筋交感神経電気刺激による末梢組織への糖取込みの亢進
　　佐々木寛之　(山形大学大学院医学系研究科生命環境医科学専攻)
130　災害医療と人工臓器―その役割・意義・課題の検討
　　原口　義座　(国立病院機構災害医療センター外科)
131　パンデミックと人工臓器―インフルエンザパンデミック対策を振り返って
　　原口　義座　(国立病院機構災害医療センター外科)
132　心房細動治療用冷却新デバイス開発の試み
　　古賀　千尋　(東北大学大学院医工学研究科)
133　壁厚制御された PVA-H 血管バイオモデルの開発
　　清光　千早　(東北大学大学院医工学研究科医工学専攻)

JSAO2010

第48回日本人工臓器学会大会

The 48th Annual Meeting of the Japanese Society for Artificial Organs

Japanese Originality for Tommorow

□ **会　　期**　平成21年11月18日（木）・19日（金）・20日（土）

□ **会　　場**　仙台国際センター
仙台市青葉区青葉山

□ **大 会 長**　山家智之
（東北大学加齢医学研究所　心臓病電子医学分野　教授）

□ **実行委員長**　齋木佳克
（東北大学大学院医学系研究科　心臓血管外科　教授）

大会事務局
〒980-8575　仙台市青葉区星陵町4-1
東北大学加齢医学研究所　心臓病電子医学分野
Tel: 022-717-8517　Fax: 022-717-8518
Email: jsao2010@idac.tohoku.ac.jp
〔大会当日直通〕
Tel: 022-234-8611（11月18日～20日）

133　壁厚制御されたPVA-H血管バイオモデルの開発

[1]東北大学大学院医工学研究科医工学専攻、[2]東北大学大学院工学研究科、[3]東北大学流体化学研究所

清光 千早[1]、小助川 博之[2]、橋田 葉子[3]、太田 信[3]

血管内治療は脳血管疾患および循環器系疾患に対する低侵襲な治療法として注目されている．しかしながら，術者は高度な技術と経験を必要とすることから，モデル (バイオモデル) が治療のトレーニングに有効であると考えられている．特に，実際の血管に近い形状と力学的特性を持った血管モデルは，血管内治療用デバイスの技術開発や術前診断等にも利用できる他，in vitro での血流解析法への貢献が期待されている．このような血管バイオモデルの材料として，Poly (vinyl alcohol) Hydrogel (PVA-H) が注目されている．PVA-H は高い透明性を示すゲルであるため挿入されたデバイスの状態を直接視認できること，低い表面摩擦抵抗を有していることから治療デバイスの操作性が体内での操作性と非常に似せることが可能なことや，化学的構造と濃度を調節することで血管に近い力学的特性を示していることから血管の挙動を再現できることなどの特長を持っている．このような弾性率を有する場合，壁厚はカテーテルのトラッカビリティの再現および血管の拍動を再現する上で特に重要となるが，PVA-H 血管バイオモデルの厚さを制御する加工法は報告されていない．そこで筆者らは Dip-Coating 法に注目した．Dip-Coating 法は材料を溶かした溶液に基板を浸漬し，一定の速度で引き上げることで基板表面に一定の厚さを持つ薄膜を形成する成膜法である．本研究では Dip-Coating 法を用いて PVA-H の薄膜を作成し，膜厚の測定を行った．この結果，薄膜と基板の引き上げ速度および PVA 溶液の濃度との間に一定の相関性があることが示唆された．またチューブ形状の PVA-H 試料を作成し，その壁厚を測定した．この結果，チューブ形状の PVA-H の壁厚を一定の精度で制御できることが示唆された．これらの結果から，壁厚の制御された PVA-H 血管バイオモデルの開発が可能であると考えられる．

134　組織工学的に皮下で作製した心臓弁付き Conduit (Biovalve) の大動脈系自家移植による性能評価

[1]国立循環器病研究センター人工臓器部、[2]国立循環器病研究センター生体医工学部、[3]京都府立医科大学附属病院心臓血管外科、[4]関西大学システム理工学部

武輪 能明[1]、中山 泰秀[2]、山南 将志[3]、花田 徹[1,3]、安藤 政彦[1,3]、齋藤 友宏[1]、松井 悠一[4]、神田 圭一[3]、夜久 均[3]、田地川 勉[4]、大場 謙吉[4]、妙中 義之[1]、巽 英介[1]

【目的】我々は人工物を体内に留置した際に起こる結合組織によるカプセル化反応を組織工学に応用し、皮下などの体内を組織構築の場（バイオリアクター）にして自己組織からなる移植片を作製するという新しい生体内組織形成技術 (In body tissue architecture technology) を開発している。これまで本技術を用いて心臓弁付き Conduit（Biovalve）を作製し、肺動脈弁位に移植し評価してきた。今回、大動物（成ヤギ）を用いた大動脈系自家移植実験に成功したので報告する。【方法】Biovalve の鋳型はアクリル製で、Valsalva 洞状の膨らみを持つ凹型と開口状態の三葉弁形状で合致する凸型から成り、両者を接合後、成ヤギ背部の皮下に埋入して 8 週間後摘出した。鋳型を抜去して 3 つの薄い弁葉と Valsalva 洞状形態を持つ Conduit 型の Biovalve が得られ、これを人工血管に組み込んだグラフトを用いて手術的に左室心尖脱血、下行大動脈送血の左心バイパス（Apico-aortic bypass）を作成し、動脈圧負荷がかかる状態で Biovalve の性能を評価した。【結果】術直後の血管造影でバイパスグラフトの血流は良好であった。術後 4 週間現在、動脈圧 100-150 mmHg、バイパス流量 2.5-4 L/min の条件下でも問題なく経過している。経胸壁エコーで Biovalve 弁葉の可動性は良好で狭窄や逆流もなく弁輪径の拡張も認めていない。【結論】本技術にて煩雑な生体外での細胞操作や無菌室などの設備を必要とせずに設計通り機能的な心臓弁の作製が可能で、高圧系でも自己弁に近い高い性能を持つことが示された。Biovalve は自家移植が可能で感染や免疫反応の心配が少なく、また、自己内膜組織の形成による抗血栓性や耐久性の向上も期待されることから、将来有望な、大動脈弁置換や大動脈根部置換などの移植グラフとなることが期待される。また、本研究で用いた Apico-aortic bypass は、高圧系での大動脈弁機能評価のための有効な慢性大動物実験モデルであり、今後の Translational research の推進にも大きく寄与するものと考えられる。

（添付４）研究発表に関する資料

信太宗也，小助川博之，橋田葉子，太田 信，“血管バイオモデル内流れのPIV計測のための疑似血液流体開発,” 日本流体力学学会年会 2010, 2010年9月9-11日 pp. 217

ISSN 1342-8004

日本流体力学会誌
「ながれ」29 巻別冊

日本流体力学会年会 2010

講　演　要　旨　集

Proceedings of 2010 Annual Meeting,
Japan Society of Fluid Mechanics

2010 年 9 月 9 日 (木) ～9 月 11 日 (土)
北海道大学 札幌キャンパス

日本流体力学会

10：50－12：30 (第2日目：会場5)　宇宙・惑星（1）　　**座長：松田　卓也(中之島科研)**

14：30－16：10 (第2日目：会場5)　宇宙・惑星（2）　　**座長：横山　央明(東大地球惑星)**

16：40－18：00 (第2日目：会場5)　宇宙・惑星（3）　　**座長：松元　亮治(千葉大)**

(9月10日)

■ 会　場　6（E311教室）■

9：00－10：20 (第2日目：会場6)　生体の流れ（1）　　**座長：関　眞佐子(関西大)**

血管バイオモデル内流れのＰＩＶ計測のための疑似血液流体開発

Development of Blood-Mimicking Fluid for Particle Image Velocimetry of Flow in Vascular Biomodel

○ 信太宗也 1，東北大医工学，仙台市青葉区片平 2－1－1，shida@biofluid.ifs.tohoku.ac.jp:
小助川博之 2，東北大工学，仙台市青葉区片平 2－1－1，hiro-kosuke@biofluid.ifs.tohoku.ac.jp:
橋田葉子 3，東北大流体研，仙台市青葉区片平 2－1－1，hashiday@tech.ifs.tohoku.ac.jp:
太田　信 4，東北大流体研，仙台市青葉区片平 2－1－1，ohta@biofluid.ifs.tohoku.ac.jp:
Shuya Shida1, Tohoku University, 2-1-1 Katahira Aoba-ku Sendai, 980-8577, Japan
Hiroyuki Kosukegawa, Tohoku University, 2-1-1 Katahira Aoba-ku Sendai, 980-8577, Japan
Yoko Hashida, Tohoku University, 2-1-1 Katahira Aoba-ku Sendai, 980-8577, Japan
Makoto Ohta, Tohoku University, 2-1-1 Katahira Aoba-ku Sendai, 980-8577, Japan

An in-vitro work fluid to apply to Poly (vinyl alcohol) hydrogel (PVA) model integrated in a circulation system are developed using glycerol. The index of refraction of the fluid is matched to that of PVA model and the model is connected to the circulation system with a pulsatile pump. The viscosity can also be changeable for matching the blood. Since the compliance of PVA model is similar to the arterial wall, the circulation system with PVA model will be helpful for comparison of flow dynamics in rigid wall or for evaluation of medical devices such as stent or coil touching on the artery. These topics are also strong relationship with the rupture of cerebral aneurysm that usually causes subarachnoidal hemorrhage (SAH) and sever morbidity.

1．背景

くも膜下出血等の致命的な症状を引き起こす脳動脈瘤の破裂は，血行動態と密接な関係があるとされている[1]．また瘤の治療に血管内治療がその低侵襲性から注目を浴びており，血管内治療で用いられる医療デバイスの効果が数値流体手法や生体外循環バイオモデル内流れの Particle Image Velocimetry (PIV)[2]によって解析されている．しかしながら，血管壁の動態や医療デバイスと血管壁表面との相互作用は，多くの場合において考慮されてこなかった．

近年，拍動による血管壁の動きの再現を目指した連成シミュレーション解析の評価や，医療デバイスが血管壁に与える影響評価等のために，壁のコンプライアンスと挙動とを同時に再現できるバイオモデルでの PIV 計測が必要と考えられている．

Poly (vinyl alcohol) (PVA) gel を用いたバイオモデルは太田らによって開発され[2]，壁のコンプライアンスを生体の血管の初期歪み時におけるコンプライアンス値と同様な値に似せることが可能であること，医療デバイスと接触した場合の表面摩擦係数が生体の血管と同様なことや，透明であるため医療デバイスを視認して評価をすることが可能なことから注目をされている．そこで，PVA モデルで PIV が可能になれば，医療デバイスの挙動を生体外でより忠実に再現でき，評価することができると考えられる．

そこで本研究では，作動流体の屈折率と動粘度を同時に適切な値に調整し測定を試みたので，報告する．

2．実験方法

2.1　PVA 動脈瘤バイオモデルの作成

蒸留水と Dimethyl sulfoxide の混合溶媒に PVA を加えた．撹拌しながら 100℃で 2 時間加熱し，PVA を溶解させた．PVA 溶液を放冷後，脳動脈石膏モデルを設置したアクリル型に流し込み，-30℃で 24 時間冷却させた．

2.2　屈折率と粘度測定による作動流体の選定

Gly 水溶液，及び NaI 水溶液の屈折率測定には，手持屈折計を用いた．また，粘度は，振動式粘度計を用いて測定した．

ここで動粘度は，別に測定した密度を用いて算出した．さらに，Gly と NaI 55 wt %水溶液の混合溶液(Gly-NaI)についても同様に屈折率，粘度の測定を行った．

2.4　PIV 計測システム

Gly-NaI を作動流体とし，トレーサ粒子を添加後，粒子画像を取得し，PIV 解析を行った．光源には波長 532 [nm]の 1[mm]厚さレーザシートを用い，粒子画像を高速度カメラで取得した．

3．結果および考察

3.1　作動流体の屈折率及び動粘度

屈折率測定の結果，PVA gel の屈折率範囲は，22℃で 1.464 から 1.470 となった．一方，Gly 水溶液，NaI 水溶液の屈折率は，混合割合に対して線形的に上昇し，PVA gel の屈折率範囲を含む値に調整可能であることが分かった．また，Gly-NaI について屈折率と動粘度を測定した結果，PVA に適切な屈折率を保ちつつ，作動流体の動粘度を幅広い値の範囲で設定できることが分かった．

3.2　粒子画像及び PIV 解析の適用

Gly-NaI (65 : 35, vol. %)を作動流体とした時の，粒子画像とその PIV 計測適用結果をみると，トレーサ粒子の散乱光の歪みや，モデルと流体の界面の強い散乱光はほとんど見られず，壁面近傍の速度ベクトルも取得可能であることがわかった．

4．結言

PVA モデル内流れへの PIV 計測適用について，粒子画像の取得が可能であることから，PIV 計測が可能であることが示唆された．

参考文献

(1) A. Mantha, C. Karmonik, G. Benndorf, C. Strother, and R. Metcalfe: Hemodynamics in a Cerebral Artery before and after the Formation of an Aneurysm, J. Neuroradiol, 27, 1113/1118 (2006)
(2) T. T. Nguyen, Y. Biadillah, R. Mongrain, J. Brunette, J.-C. Tardif, and O. F. Bertrand: A Method for Matching the Refractive Index and Kinematic Viscosity of a Blood Analog for Flow Visualization in Hydraulic Cardiovascular Models, Biomechanical Eng., 126, 529/535 (2004)
(3) M. Ohta, A. Handa, H. Iwata, D. A. Rüfenacht, and S. Tsutsumi: Poly-vinyl alcohol hydrogel vascular models for in vitro aneurysm simulation: the Key to low friction surfaces, Technology and Health Care, 12, 225/233 (2004)

（添付５）研究発表に関する資料

S. Shida, H. Kosukegawa, K. Kuroki, M. Ohta, “Development of Blood-Mimicking Fluid with Adjusted Refractive Index and Kinematic Viscosity for Applying to Particle Image Velocimetry,” 6th World Congress of Biomechanics, Aug.1-6, 2010, pp. 536

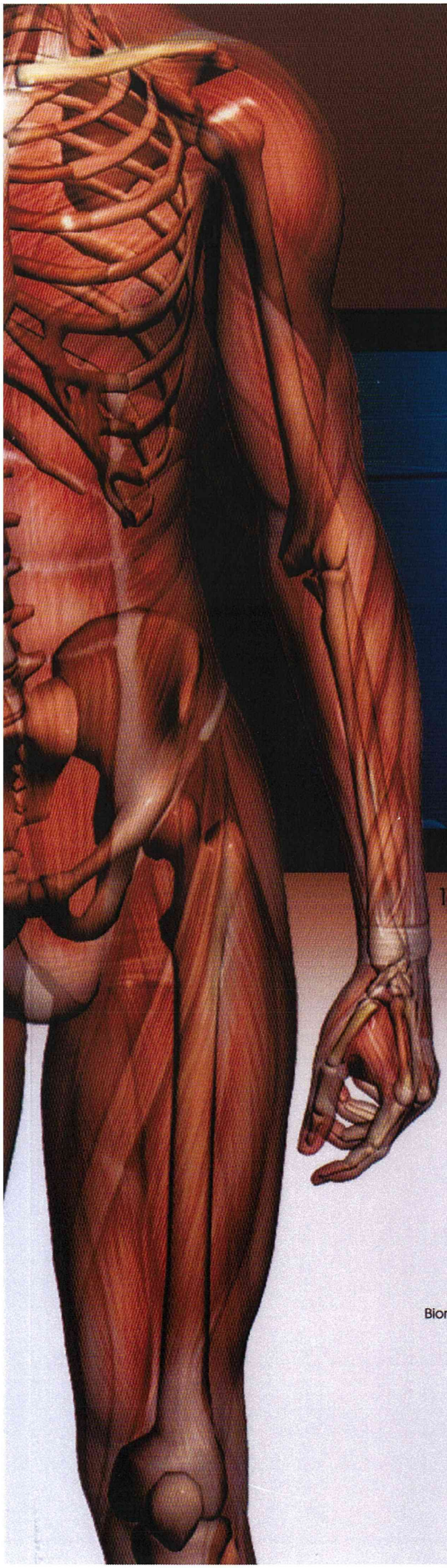

6th World Congress of Biomechanics

Abstracts

In conjunction with

14th International Conference on Biomedical Engineering (ICBME)

&

5th Asian Pacific Conference on Biomechanics (APBiomech)

1 - 6 August 2010
Singapore Suntec Convention Centre

Jointly Organised by

BES SINGAPORE
Biomedical Engineering Society (Singapore)

Global Enterprise for Micromechanics and Molecular Medicine

NUS National University of Singapore
National University of Singapore

Endorsed By

IFMBE
International Federation for Medical and Biological Engineering

D2-D-T6.2: **Track 6.2: Modeling & Simulation**
Date: **Tuesday, 3 August 2010**
Time: **1630 - 1815 hrs**
Room: **301**
Session Chair(s): **Ning Gangmin, Hideo Utsuno**

1630 - 1645 hrs **WCB-A00222-00605** **D2-D-T6.2-01**
Validation of Idealized Knee Joint Models - An in vivo Study
Michael Skipper Andersen, John Rasmussen, Dan Ramsey, Daniel Benoit

1645 - 1700 hrs **WCB-A00566-00829** **D2-D-T6.2-02**
Research on the Measurement of the Propagation Velocity and the Reflection Ratio of Pulse Waves in the Blood Vessel.
Hideo Utsuno, Hironori Sato, Shin-suke Yamashita, Hiroshi Matsuhisa, Keisuke Yamada

1700 - 1715 hrs **WCB-A00556-01488** **D2-D-T6.2-03**
Development of Blood-Mimicking Fluid with Adjusted Refractive Index and Kinematic Viscosity for Applying to Particle Image Velocimetry
Shuya Shida, Hiroyuki Kosukegawa, Kanjyu Kuroki, Makoto Ohta

1715 - 1730 hrs **WCB-A00889-02282** **D2-D-T6.2-04**
Simulation of Blood Pressure Wave Propagation in a Vessel by One-dimensional Model
Gangmin Ning, Yuexian Gong, Shijin Gong, Qing Pan, Jing Yan, Axel R. Pries

1730 - 1745 hrs **WCB-A00727-02235** **D2-D-T6.2-05**
Experimental Investigation of Blood Flow in the Vertebral Artery Bifurcation
Guangyu Zhu, Qi Yuan, Zhen Chen

1745 - 1800 hrs **WCB-A01210-02104** **D2-D-T6.2-06**
Novel System to Quantify Thromboembolic Potential of Mechanical Heart Valves
Sivakkumar Arjunon, Neelakantan Saikrishnan, John Culp, Lakshmi Dasi, Jelena Vukasinovic, Taylor Jones, Sahaja Bandari, Ari Glezer, Ajit Yoganathan

1800 - 1815 hrs **WCB-A00474-00653** **D2-D-T6.2-07**
Influence of Soft Tissues on Propagation of Ultrasonic Lamb Waves in Synthesised Soft Tissue-Bone Phantoms
Jiangang Chen, Li Cheng, Zhongqing Su, Ling Qin

WCB-A00417-00554

Automated Classification of Neurodegenerative Diseases

Nivedita CHAUDHARY
Biomedical Instrumentation, Birla Institute of technology, Ranchi/Jharkhand, India

Neurodegenerative disease occurs due to deterioration of cells specially the myelin sheath of the neurons; of brain, spinal cord, and peripheral nerves. The economic and social burden of neurodegenerative diseases is massive and rising too rapidly. Among several of different neurodegenerative disorders present work is focused on three most common; Alzheimer's disease, Parkinson's disease, and Huntington's disease. Although most consistent risk factor for developing a neurodegenerative disorders is increasing age, it has been observed that the symptoms of all three diseases overlap with each other, clinically and pathologically. Therefore, their practical classification is quite challenging and thus need an automated tool to classify them. In the present model, backpropagation artificial neural network (ANN) has been designed to classify neurodegenerative disorders according to their symptoms. The 27:70:3 architecture of ANN has been used to predict the clinical outcome from the complex overlapped symptoms that are routinely available to clinicians. The model has found to be effective in differentiating the different types of focused diseases with an overall performance of 96.42%.

WCB-A00510-02939

Estimation of Lower Limb Joint Angles During Walking Using Extended Kalman Filtering

Diana YOUNG[1]; Sofia D'OREY[2]; Roedolph OPPERMAN[3]; Christopher HAINLEY[3]; Dava NEWMAN[3]
1. *Biomechatronics Group, Media Laboratory, Massachusetts Institute of Technology, Cambridge, MA, United States*
2. *Instituto Superio Tecnico, Lisbon, Portugal*
3. *Aeronautics and Astronautics, Massachusetts Institute of Technology, Cambridge, MA, United States*

In order to evaluate the performance of an extended Kalman filter (EKF) for the estimation of lower limb joint angles generated during human walking, a pilot study is conducted using commercial inertial measurement units (IMUs) to capture 3D acceleration and angular velocity data produced by the leg during level ground, stair ascent, and stair descent walking. The inertial data from three IMUs, one mounted on each lower limb segment, are input to an EKF to estimate sagittal and coronal angles of the individual limb segments and the corresponding knee and ankle joint angles. This method is evaluated against the standard method performed using optical motion capture and inverse kinematics software. Results from three subjects are reviewed, and the promising potential of this technique for realtime applications is discussed.

WCB-A00534-00773

Image Correlation Spectroscopy for Microrheology of Soft Materials

Nicholas Agung KURNIAWAN[1]; Chwee Teck LIM[2,3]; Raj RAJAGOPALAN[4,5]
1. *NUS Graduate School for Integrative Sciences and Engineering, National University of Singapore, Singapore*
2. *Department of Mechanical Engineering, National University of Singapore, Singapore*
3. *Division of Bioengineering, National University of Singapore, Singapore*
4. *Department of Chemical and Biomolecular Engineering, National University of Singapore, Singapore*
5. *Chemical and Pharmaceutical Engineering Program, Singapore-MIT Alliance, National University of Singapore, Singapore*

Image correlation spectroscopy (ICS) is a family of biophysical methods that has been used to perform spatiotemporal measurements on biological materials, especially cells. Some of the early uses of ICS include quantifying spatial distribution, aggregation state, diffusion coefficient, as well as flow and interaction of cellular protein molecules. In the present work, we show, in addition to these original applications, how ICS can be used to perform microrheological measurement of complex, viscoelastic materials. We test the method, which we call ICS-μR, on Newtonian fluids as well as complex, viscoelastic fluids with different viscosities and viscoelastic behaviors. Comparison of ICS-μR results with reported data from the literature as well as results from conventional rheology measurements yield excellent agreement. Furthermore, we develop a special technique for extracting mean-squared displacements of tracer particles in the samples from image correlation data; the technique successfully reproduces previously published experimental data on a wide range of soft materials displaying a broad scale of scaling behaviors. This technique can be applied to improve the accuracy of other microrheological measurements and can potentially offer new insights on the power-law behaviors of materials. The possibility to combine spatiotemporal assessment and time- and length-scale dependent microrheological measurements from images of fluorescent molecules makes ICS-μR a prospective tool in many biophysical applications.

WCB-A00545-00827

Researches on Spatio-temporal Expressions of Intestinal Pressure Activity Acquired by the Capsule Robot

Rongguo YAN[1]; Xudong GUO[1]; Guozheng YAN[2]
1. *School of Medical Instrument and Food Engineering, University of Shanghai for Science and Technology, Shanghai, China*
2. *Department of Information Measurement Technology and Instruments, Shanghai Jiaotong University, Shanghai, China*

AIM: To give researches on the spatio-temporal expressions of the intestinal pressure activity.

METHODS: The intestinal pressure activity was acquired by using a capsule robot invented for functional diagnosis of human gastrointestinal diseases, which collected intestinal physiological parameters as it propelled itself within the gastrointestinal tract.

RESULTS: a series of different contraction types were systematically analyzed to form the corresponding spatio-temporal expressions of the intestinal pressure activity including (1) standing contractions, (2) propagating segmental contractions, and (3) pendular contractions.

CONCLUSIONS: Spatio-temporal expressions could provide a method for visualizing a temporally evolving and spatially varying intestinal pressure activity.

WCB-A00556-01488

Development of Blood-Mimicking Fluid with Adjusted Refractive Index and Kinematic Viscosity for Applying to Particle Image Velocimetry

Shuya SHIDA[1]; Hiroyuki KOSUKEGAWA[2]; Kanjyu KUROKI[3]; Makoto OHTA[3]
1. *Graduate School of Biomedical Engineering, Tohoku University, Sendai, Japan*
2. *Graduate School of Engineering, Tohoku University, Sendai, Japan*
3. *Institute of Fluid Science, Sendai, Japan*

BACKGROUND AND PURPOSE: Blood vessel disease such as cerebral aneurysm is life-threatening disease and as large cause of death as cancer in many countries. In endovascular therapy of cerebral aneurysms using medical devices such as coil or stent, hemodynamics in aneurysm is related to thrombosis formation in aneurysm and the repairing. Then, it may be important to make realistic blood flow pattern in in-vitro cerebral aneurysms such as biomodel (in-vitro functional model of aneurismal blood vessel) to treat aneurysm as well as check medical devices of the therapy. The Particle Image Velocimetry (PIV) method is one of the strongest tools for measurement of flow in biomodel and requires a match of the refractive index between material of biomodel and working fluid in order to eliminate optical problems such as image distortion. Moreover, in vascular research, the working fluid should be a mimic human blood with respect to kinematic viscosity so as to obtain realistic blood flow modeling measurements. In this research, detailed measurements of physical properties of solutions are performed to develop a method to adjust working fluid that has proper refractive index and kinematic viscosity simultaneously.

MATERIALS AND METHODS: The adjustable range of refractive index and kinematic viscosity of working fluid were measured by under the mixing aqueous solution of glycerol (glycerol aq.) and aqueous solution of NaI (NaI aq.) with various weight proportion. All properties of the solutions were measured on the same day at room temperature and atmospheric pressure. The refractive index to light of a fluorescent and dynamic viscosity were measured with a critical angle refractometer (R-5000, ATAGO CO., LTD., Japan) and a vibration-type viscometer (SV-10, A&D CO., LTD., Japan), respectively. And then, Kinematic viscosity is calculated form dividing the dynamic viscosity with its density.

RESULTS AND DISCUSSION: The refractive index (n) of gly. aq. and NaI aq. increase monotonically from that of distillated water values (n = 1.333) to that of glycerol value (n = 1.472) and that of NaI aq. 0.6 wt % value (n = 1.4813 ± 0.0002), respectively. This result indicates that refractive index of NaI aq. will vary in wide range compared with gly. aq. As for kinematic viscosity (ν), gly. aq. increase very slightly especially at high proportion and reach maximum value ν = 855.6 mm2/s. Meanwhile, kinematic viscosity of NaI aq. has a unique feature; the value increases to the maximal value at around 0.3 weight proportion, and decreases to minimal value at around 0.35 weight proportion, then again increases rapidly. The refractive index of the mixture, which kinematic viscosity is adjusted to blood value (3.8 mm2 / s), is in range from 1.390 to 1.472 at room temperature (21.5 ± 0.5 degrees celsius) by using the two aqueous solutions.

CONCLUSION: The mixtures have a wide range of kinematic viscosity at fixed refractive index with the method of mixing two aqueous solutions. This mixture way and the liquid could be applied as working fluid widely to various biomodels such as PVA models or silicone models.

（添付６）研究発表に関する資料

Shuya Shida, Hiroyuki Kosukegawa, Makoto Ohta, Development of a methodology for adaptation of refractive index under controlling kinematic viscosity for PIV, IMECE2011- 64388, Colorad, Nov. 11-15, 2011

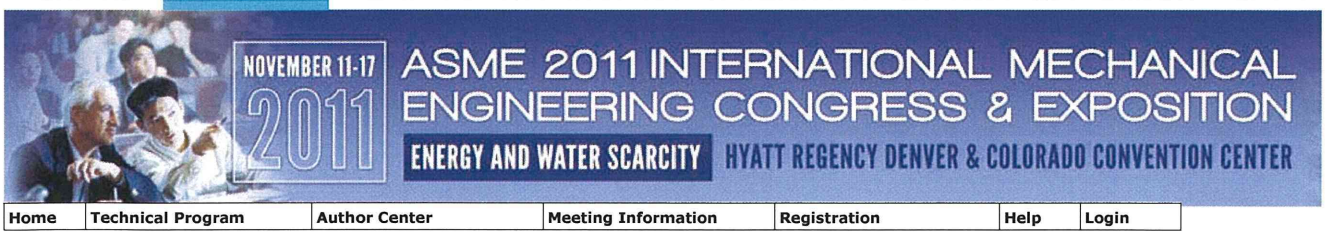

FIRST TIME USERS to the ASME Itinerary Planner
ASME Itinerary Planner
Committee Meetings
Energy Grand Challenge
Exhibits/Sponsorships
Honors Assembly
Hotel Reservations
Keynote Event
List of Organizers
Plenary Speakers
Press Room
Short Course
Special Events
Technical/Guest Tours
Technical Program

Have Questions? Contact Us.

Acceptance Notification, Technical Content, etc.
Volunteer Organizers

Registration Information
imece@asme.org

Hotel Information
Melissa Torres

Committee Meeting Logistics
Stephen Crane

Copyright Forms
copyright@asme.org

Web Tool Support
congresshelp@asme.org

Technical Program Overview

Conference Schedule | Program Search

Note: Program is subject to change.

Expand All

- **Track 1 Energy Water Nexus** Expand All Topics In Track
- **Track 2 Energy Systems Analysis, Thermodynamics, and Sustainability** Expand All Topics In Track
- **Track 3 Combustion Science and Engineering** Expand All Topics In Track
- **Track 4 NanoEngineering for Energy** Expand All Topics In Track
- **Track 5 Nano and Micro Materials, Devices and Systems** Expand All Topics In Track
- **Track 6 Microsystems Integration** Expand All Topics In Track
- **Track 7 Nanoengineering for Medicine and Biology** Expand All Topics In Track
- **Track 8 Biomedical and Biotechnology Engineering** Expand All Topics In Track

  Track Organizer: Ahmed Al-Jumaily, *Institute of Biomedical Technologies (IBtec), Auckland University of Technology (AUT)*

  Track Co-Organizer: Sara Wilson, *University of Kansas*

  Track Co-Organizer: Ram Devireddy, *LSU*

  Track Co-Organizer: Erol Ulucakli, *Lafayette College*

  - **8-1 Biomedical and Biotechnology Plenary Presentation**
  - **8-2 BioMEMS, Micro and Nano Systems in Medicine and Biology**
  - **8-3 Vibration and Acoustics in Biomedical Applications**
  - **8-4 Application of Composites in Biomaterials and Bioengineering**
  - **8-5 Viscoelasticity of Biological Tissues**
  - **8-6 Dynamics and Control of Biomechanical Systems**
  - **8-7 Bioengineering and Clinic Applications**
  - **8-8 Analysis of Trauma Due to Blast, Ballistics, and Impacts**
  - **8-9 Biomedical Heat Transfer, Transport Phenomena and Fluid Mechanics**

    Topic Organizer: Erol Ulucakli, *Lafayette College*

    Topic Co-Organizer: Franz-Josef Kahlen, *University of Cape Town*

    - 8-9-1 Experimental Heat Transfer 1 *(Technical Session)*
    - 8-9-2 Experimental Heat Transfer 2 *(Technical Session)*
    - 8-9-3 Computational Heat Transfer *(Technical Session)*
    - 8-9-4 Biomedical Fluid Dynamics *(Technical Session)*

      Session Schedule: Wednesday, November 16, 2011 **04:30 PM-06:00 PM**

      Session Sponsors: Biomedical Heat Transfer

      Session Organizer: Erol Ulucakli, *Lafayette College*

      Session Co-Organizer: Aneesha Gogineni, *Wichita State University*

      Session Co-Organizer: Tiruvadi Ravigururajan, *WSU, ME*

IMECE2011-64621	Flow Through Stented Arteries - A Review	Technical Publication
IMECE2011-64388	Development of a Methodology for Adaptation of Refractive Index under Controlling Kinematic Viscosity for PIV	Technical Publication
IMECE2011-63608	Nemerical Hemodynamics Analysis of Stented Cerebral Artery	Technical Publication
IMECE2011-62986	Effects of high shear rate on thrombus formation process on pipe orifice flows	Technical Publication

  - **8-10 Computational Modeling and Device Design**
  - **8-13 Processing and Characterization of Bio-inspired and Biomimetic Materials**
- **Track 9 Advances for Process Industries** Expand All Topics In Track
- **Track 10 Heat and Mass Transport Processes** Expand All Topics In Track
- **Track 11 Fluids & Thermal Systems** Expand All Topics In Track
- **Track 12 Mechanics of Solids, Structures and Fluids** Expand All Topics In Track
- **Track 13 Dynamic Systems and Control** Expand All Topics In Track
- **Track 14 Mechatronics & Intelligent Machines** Expand All Topics In Track
- **Track 15 Vibration, Acoustics & Wave Propagation** Expand All Topics In Track
- **Track 16 Design and Manufacturing** Expand All Topics In Track

Proceedings of the ASME 2011 International Mechanical Engineering Congress & Exposition
IMECE2011
November 11-17, 2011, Denver, Colorado, USA

IMECE2011-64388 - DRAFT-

DEVELOPMENT OF A MTHODOLOGY FOR ADAPTATION OF REFRACTIVE INDEX UNDER CONTROLLING KINEMATIC VISCOSITY FOR PIV

Shuya SHIDA
Graduate School of Biomedical Engineering, Tohoku University
Sendai, Miyagi, Japan

Hiroyuki KOSUKEGAWA
Graduate School of Engineering, Tohoku University
Sendai, Miyagi, Japan

Makoto OHTA
Institute of Fluid Science, Tohoku University
Sendai, Miyagi, Japan

ABSTRACT

Blood vessel diseases such as ischemic cardiac disease or cerebral aneurysm are life-threatening disorders and as large a cause of death as cancer in many countries. The rupture of a cerebral aneurysm usually causes subarachnoidal hemorrhage the mortality of which is very high. Previous studies have proved that the genesis and growth of aneurysm are related to hemodynamics. Especially, in endovascular therapy for cerebral aneurysms using medical devices such as coils or stents, hemodynamics in an aneurysm are related to thrombosis formation in the aneurysm and to its repair. In vascular research using a biomodel (blood vessel phantom with mechanical properties similar to a human artery) for treating cerebral aneurysm, the working fluid, termed Blood-Mimicking Fluid (BMF), should mimic human blood with respect to viscosity so as to obtain realistic blood flow modeling in *in vitro* measurements. Moreover, refractive indices of BMF must be adjusted to fit biomodel materials because the materials used for Particle Image Velocimetry, one of the best tools for measurement of flow, have various refractive indices. For simultaneous adjustment of the two parameters, i.e. kinematic viscosity and refractive index, an aqueous mixture of glycerol and sodium iodide has been used in previous research. In this paper, we develop a systematic way to precisely find the two targeted parameters of BMF by showing the measurement values of the refractive index and the viscosity of the two aqueous solutions.

The refractive index to light of fluorescent was measured with a critical angle refractometer while temperature of sample was also measured. And a vibration-type viscometer was used to obtain the dynamic viscosity under the same condition as refractive index measurement. These measurements were carried out at room temperature and pressure, respectively.

As a result of detailed measurements at various proportions, refractive indices of the aqueous solution of glycerol (Gly. aq.) increase monotonically. On the one hand, the kinematic viscosity of Gly. aq. increases very slightly with its proportion and that of the aqueous solution of sodium iodide (NaI aq.) exhibits unique behavior. The results of combining Gly. aq. and NaI aq. indicate that the mixture has a wide range of kinematic viscosity, including the value of blood (around 3.8 mm^2/s), at the targeted refractive index.

In conclusion, this mixing method is useful for BMF preparation with the adjustment of refractive index and kinematic viscosity.

NOMENCLATURE

C_j	The number of molecules per volume unit of a component j
c	The electrolyte molar concentration
G_{12}	The activation energy of glycerol aqua
M	Molar mass
M_0	Molar mass of solvent
N_A	The Avogadro number
n	Refractive index
n_s	Total salvation number
Re	Reynolds number
R^2	Determination coefficient
T	Absolute temperature
W_0	Womersley number
w	Weight proportion
$\overline{\alpha}_j$	Mean polarizability per volume unit of a component j
$\overline{\alpha}_0$	Mean polarizability per volume unit of solvent
$\overline{\alpha}_+$	Mean polarizability per volume unit of cation
$\overline{\alpha}_-$	Mean polarizability per volume unit of anion

μ Dynamic viscosity
μ_{gl} Dynamic viscosity of glycerol
μ_{wa} Dynamic viscosity of distillated water
ν Kinematic viscosity
ρ Density (specific weight) of the solution
χ The molar fraction

1. INTRODUCTION

Blood vessel diseases such as ischemic cardiac disease or cerebral aneurysm are life-threatening disorders and as large a cause of death as cancer in many countries. The rupture of a cerebral aneurysm usually causes subarachnoidal hemorrhage, the mortality of which is very high. Previous studies have proved that the genesis and growth of aneurysms are related to hemodynamics. Especially, in endovascular therapy for cerebral aneurysms using medical devices such as coils or stents, hemodynamics in an aneurysm are related to thrombosis formation in the aneurysm and to its repair. However, *in vivo* hemodynamics are difficult to be measured quantitatively and an *in vitro* circulation system or Computational Fluid Dynamics (CFD) can be utilized.

CFD study is carried out for measurement of hemodynamics. In particular, Fluid-Structure Interaction (FSI) analysis is utilized to reproduce hemodynamics more precisely with a model of blood wall movement [1-3], whereas an *in vitro* measurement system is also employed because it can confirm the CFD results. Therefore, it may be important to create a realistic blood flow pattern in *in vitro* cerebral aneurysms such as a biomodel (blood vessel phantom with mechanical properties similar to a human artery) to treat aneurysms and to check therapeutic medical devices as well as to validate flow quantitatively.

In vascular research using a biomodel, the working fluid, termed Blood-Mimicking Fluid (BMF), should mimic human blood with respect to dynamic or kinematic viscosity so as to obtain realistic blood flow modeling in measurements. Fluid viscosity affects fluid phenomena or parameters such as Reynolds number (*Re*), Womersley number (*Wo*), shear stress, momentum flux and viscous dissipation. Particularly, *Re* is important for maintenance of the flow similarity. Also, the similarity rule in fluid dynamics is not so applicable to vascular research with medical devices because the devices have a real scale size to fit human organs. Additionally, unsteady flow conditions require that *Wo* matches *in vivo* blood flow in order to prevent a flow phase difference. Thus, dynamic viscosity (μ) or kinematic viscosity (ν) should be similar to the value of blood ($\mu \sim 4.0$ mPa·s, $\nu \sim 3.8$ mm^2/s in many cases (*e.g.* [4]) for in-vitro measurement of blood flow. Besides, it is good for experimental studies that the viscosity of BMF can have a pathological value from 2 to 10 mPa·s caused by hematocrit change or thrombosis formation.

Moreover, Particle Image Velocimetry (PIV), one of the best tools for measurement of flow in a biomodel, needs a refractive index (n) match between model material and BMF to improve the accuracy of the measurements.

The biomodel materials used for the PIV method have various refractive indices. Budwig et al. summarized the refractive indices commonly used materials such as glass (Pyrex) (n = 1.47 to 1.49), and acrylic (n = 1.49) [5]. Especially, silicone elastomer (n = 1.40 to 1.44) has been widely used, because of its transparency, inertness, and availability (*e.g.* [6-9]).

Meanwhile, poly (vinyl alcohol) (PVA) gel has been proposed for use in the development of blood vessel biomodeling by Ohta et al. [10]. They have reported that a biomodel made of PVA gel shows good transparency and lower surface friction compared with a biomodel made of silicone elastmer. Moreover, Kosukegawa et al. found that the dynamic viscoelasticity of PVA gel was similar to that of blood vessels [11]. Thus, PVA gel has attracted a great deal of interest as a biomodel material. Therefore, it is now necessary that refractive indices fit several transparent materials to independently measure the flow in the biomodels with several viscosities.

To a fit refractive index to the biomodels, an aqueous solution of glycerol (Gly. aq.) (*e.g.* [6-9, 12])or an aqueous solution of NaI (NaI aq.) (*e.g.* [13, 14]) has been widely used in the literature as a BMF for vascular studies with PIV. However, the refractive indices and the viscosities of these solutions depend on the concentration of the solutions.

A method in which Gly. aq. and NaI aq. were combined to simultaneously achieve the proposed refractive index and viscosity has been suggested. Sankovic et al. carried out PIV measurement of flow in an acrylic model with a mixture of two aqueous solutions of which the refractive index and viscosity were adjusted simultaneously [15]. Yusif et al. demonstrated refractive index matching to that of a silicone model for developing a BMF with a targeted dynamic viscosity by adding NaI to Gly. aq.[16]

This method may have potential to handle several refractive indices and viscosities, independently, because the refractive index of Gly. aq. has a linear relation to the mixture ratio, while the viscosity of Gly. aq. has a logarithmic relation to the mixture ratio [17]. Therefore, the refractive index and the viscosity in the solution with various concentrations should be measured.

In this paper, we show the measurement values of the refractive index and viscosity of a mixed solution with various concentrations and reveal that the values could have a wide range to match various model materials. A simple way to precisely find a targeted viscosity and refractive index of BMF is introduced.

2. MATERIALS AND METHODS

2.1. Equations

A few theoretical or experimental equations are described below for discussion, including validation of results for density, refractive index, and viscosity of a solution at constant temperature and pressure (that is room temperature and atmospheric pressure in this study).

2.1.1. Equations for density and refractive index

Suppose a mixture, the refractive index of which should be given by total polarizability of components by the following equation known as the Lorenz-Lorenz formula (*e.g.* [18, 19]).

$$\frac{3}{4\pi}\frac{n^2-1}{n^2+2}=\sum_j C_j\bar{\alpha}_j \tag{1}$$

where n is the refractive index of the mixture; C is the number of molecules per volume unit; $\bar{\alpha}$ is the mean polarizability per volume unit of a component, and subscript j it presents each component of the mixture.

For an ionic solution with separated ions, the formula can be expressed with weight proportion of salt, w, by the following equation [18].

$$\frac{3}{4\pi N_A}\frac{1}{\rho}\frac{n^2-1}{n^2+2}=\frac{\bar{\alpha}_0}{M_0}+w\left[\frac{\bar{\alpha}_+ +\bar{\alpha}_-}{M}-\frac{\bar{\alpha}_0}{M_0}\left(1+n_s\frac{M_0}{M}\right)\right] \tag{2}$$

where N_A is the Avogadro number; ρ is the density (specific weights) of the solution; M is molecular mass; n_s is total solvation number; the subscript +, −, and 0 are for cation, anion and solvent, respectively.

Hence, we define function f of w from eq. (2) as follows:

$$f=\frac{1}{\rho}\frac{n^2-1}{n^2+2}=f_0+f(w) \tag{3}$$

If $\bar{\alpha}$ is expected to be the same in all proportions (w), eq. (3) would be linear with w.

2.1.2. Equations for viscosity

Referring to a previous study [20], we suppose that the dynamic viscosity of glycerol aqueous solution (Gly. aq.), μ, follows the following equation.

$$\ln(\mu)=w\ln(\mu_{gl})+(1-w)\ln(\mu_{wa})+w(1-w)G_{12}$$

$$=(-G_{12})w^2+\{\ln(\mu_{gl})-\ln(\mu_{wa})+G_{12}\}w+\ln(\mu_{wa}) \tag{4}$$

where G_{12} is the activation energy of Gly. aq.; subscripts *gl* and *wa* are for the value of glycerol and distillated water, respectively. Equation (4) indicates that $\ln(\mu)$ is the quadratic function with w.

For an aqueous electrolyte solution such as aqueous sodium iodide solution (NaI aq.), the viscosities were previously derived by various modeling [21-23] as shown in the following examples.

$$\mu=\mu_0(1+Ac^{1/2}+Bc+Dc^2) \tag{5}$$

$$\mu=\frac{\mu_0\exp(\chi E)}{1+\chi V} \tag{6}$$

where μ_0 is the viscosity of solvent; c is the electrolyte molar concentration; χ is the molar fraction; and A, B, and C are constants which represent solute structural interactions; parameters E and V are decided by free energy and hydration state, respectively. Equation (5) as well as (6) can be described as functions of w because concentrations c and χ are represented with a weight proportion, respectively. The resulting dynamic viscosity of NaI aq. will be compared using Eq. (5) and (6).

2.2. Measurements

Liquid samples were basically prepared with respect to each 0.1 weight proportion, so that the measurements could be duplicated. As for NaI aq., errors of measurements (standard deviation : SD) were derived from results obtained by three sets of measurements.

To let the reaction dissipate, the samples were kept at room temperature (22℃) for more than 2 hours. All the properties of each solution (Gly. aq., NaI aq., and mixtures) were measured on the same day at room temperature and atmospheric pressure.

2.2.1. Measurement of density

The densities of the samples were derived by their weight and volume measured by using a digital weight scale, with an accuracy of ±0.01 g, and a measurement flask (25 ml or 50 ml), respectively.

2.2.2. Measurement of refractive index

The refractive index to a fluorescent light was measured using a critical angle refractometer (R-5000, ATAGO CO., LTD., Japan), temperature of the sample also being measured. Total internal reflection occurs when a ray of light strikes a medium boundary at an angle larger than a particular critical angle with respect to the normal to the surface. Because the boundary position between light and dark varies as the relative refractive index of a sample to the prism, a refractive index of a sample is measured by observing the boundary position. The error of scale reading with the refractometer is around ±0.0005.

2.2.3. Measurement of viscosity

Dynamic viscosities of the samples were measured with a vibration-type viscometer (SV-10, A&D CO., LTD., Japan) under the same condition as refractive index measurement. An oscillator is inserted into a sample and vibrated during measurement with the viscometer. Viscosity is obtained by measuring the driving current that provides constant frequency and amplitude of vibration, since friction force acting on the oscillator is proportional to the viscosity of a sample. This viscometer displays a dynamic viscosity to within 0.01 mPa· s that is multiplied by the specific gravity of the sample.

Therefore, dividing a display value by its specific gravity gives the absolute value of dynamic viscosity. Kinematic viscosity is then calculated by dividing the absolute value by its density.

3. RESULTS

Detailed measurements of physical properties of Gly. aq., NaI aq., and mixtures of Gly. aq. and NaI aq. at various proportions were performed. All experimental data were obtained as a function of weight proportion at the temperatures shown in the graphs. Equations of fitted curves are shown in most of graphs to access the accuracy of the measurements and compare the data with those of previous studies.

3.1. Results for glycerol aqueous solution

3.1.1. Density, refractive index and value *f*

Density, refractive index, and derived values of *f* of Gly. aq. are shown in Fig. 1 to 3, respectively. The measured values and derived values in these figures are fitted by linearization as a function of gly. aq. weight proportion. The density and refractive index of gly. aq. increase monotonically from that of distilled water values (ρ = 0.9945 g/cm^3, and n = 1.333, respectively) to that of glycerol values (ρ = 1.2561 g/cm^3, and n = 1.472, respectively), and they are accurately approximated by linearization (Determination coefficient : R^2 = 0.9990, and 0.9985, respectively). Though the value *f* has a few variations at high proportions up to 0.8, whole values are approximated linearly (R^2 = 0.9919). The results for density and refractive index should be accurate based on this linear approximation.

3.1.2. Dynamic viscosity and kinematic viscosity

Vertical axis of Fig. 4 and 5 describe dynamic and kinematic viscosity of natural logarithm, respectively. They are accurately approximated by quadratic polynomial (R^2 = 0.9923, and 0.9918, respectively). These results should be credible since Eq. (4) predicts that the dynamic viscosity of the natural logarithm depends on the proportion squared. The dynamic viscosity and the kinematic viscosity of pure glycerol reach maximum values: μ = 1074 mPa· s, ν = 855.6 mm^2/s, respectively.

3.2. Results for NaI aqueous solution

As mentioned in chapter 2, all the measurements for NaI aq. were carried out in triplicate. The error bars in Figs. 6 to10 represent standard deviations of the measured values.

3.2.1. Refractive index, density, and value *f*

As for NaI aq., the resulting densities and refractive indices shown in Figs. 6 and 7 are fitted by quadratic polynomial as a function of NaI weight proportion (R^2 = 0.9994, and 0.9995, respectively). The experimentally measured density and refractive index of NaI aq. also increase monotonically to ρ = 1.793 ± 0.002 g/cm^3 and n = 1.4813 ± 0.0002 at w = 0.6, respectively. This result indicates that the refractive index of NaI aq. will vary in a wide range compared with Gly. aq. The derived values *f* of NaI aq. which are fitted by linearization are shown in Fig. 8 together with the fitted curve by Camus et al

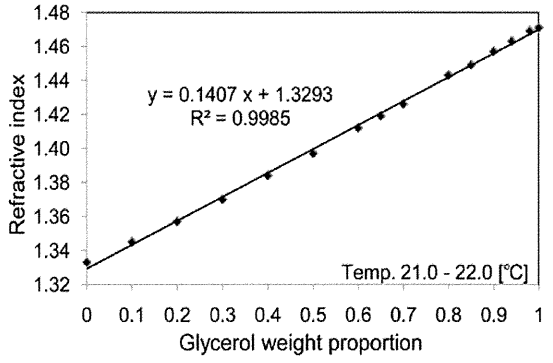

Fig. 1 Density of Gly. aq. and fitted curve by linearization as a function of glycerol weight proportion

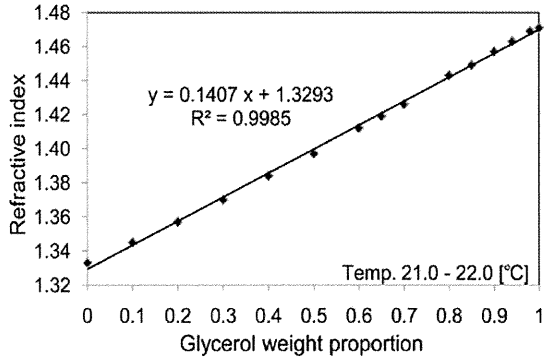

Fig. 2 Refractive index (to wavelength of fluorescent light) of Gly. aq. and fitted curve by linearization as a function of glycerol weight proportion

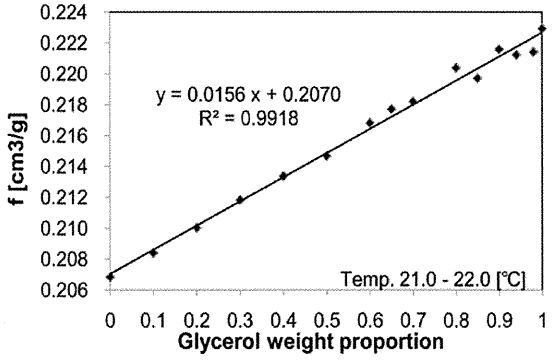

Fig. 3 Derived values of *f* with measured values of Gly. aq. and its fitted curve by linearization as a function of glycerol weight proportion

[18]. Because the equation of the present fitted curve ($f = -0.0796\ w + 0.2070$) corresponds approximately to that of the previous one ($f = -0.0773\ w + 0.2086$) [18], these results should be valid.

3.2.2. Dynamic viscosity and kinematic viscosity

The observed dynamic viscosity of NaI aq. is plotted in Fig. 9. In this figure, the present results are compared with previous results that were represented by equation (5) [22, 23] with the following constants: A = 0.01085, B = 0.0122, D = 0.01266, E = 13.35, and V = 13.82, respectively. Compared with equation (5) and (6), the present result is generally similar to the previous one with respect to increasing tendency and range. Meanwhile, the present result has a unique feature, *i.e.* the dynamic viscosity increases to the maximal value at around 0.3 weight proportion, and decreases to minimal value at around 0.35 weight proportion, then again increases rapidly.

Figure 10 shows the kinematic viscosity of NaI aq. which was derived from the above-mentioned dynamic viscosity divided by the density. Though the kinematic viscosity changes in much the same way as the dynamic viscosity, the difference between maximal and minimal values is greater than the values of kinematic viscosity, and the variation range is narrow because of the rapid increase of density with respect to weight proportion.

3.3. Results for mixtures of glycerol and sodium iodide aqueous solution

BMFs with a specific refractive index and a wide range of kinematic viscosity simultaneously were prepared by mixing Gly. aq. and NaI aq. Figure 11 shows kinematic viscosities of the mixture of Gly. aq. and NaI aq. (Gly-NaI) with the weight proportion of Gly. aq. to whole mixture weight (Gly. aq. + NaI aq.) at the targeted refractive index (1.408 and 1.425 data selected as an example). The mixtures were composed of Gly aq. (glycerol 57.0 wt %) and NaI aq. (sodium iodide 38.5 wt %) for preparing a refractive index of 1.408, and composed of Gly aq. (glycerol 69.0 wt %) and NaI aq. (sodium iodide 44.5 wt %) for preparing a refractive index of 1.425, respectively. The proportions of aqueous solutions were predicted by referring to results of previous sections. The result shown in Fig. 11 indicates that the mixtures have a wide range of kinematic viscosity at a fixed refractive index with the method of combining two aqueous solutions. The range includes the value of blood (around 3.5 to 4.0 mm^2/s)

4. DISCUSSION

This work has precisely presented the refractive index and kinematic viscosity of Gly. aq. and NaI aq. with respect to weight proportion to show an adjustment method to derive a proportion of targeted viscosity and refractive index of BMF. The results show that a mixture using the two solutions with the same refractive index has a constant refractive index and can be adjusted to various kinematic viscosities. The properties following the linear or quadric, logarithmic correlations are

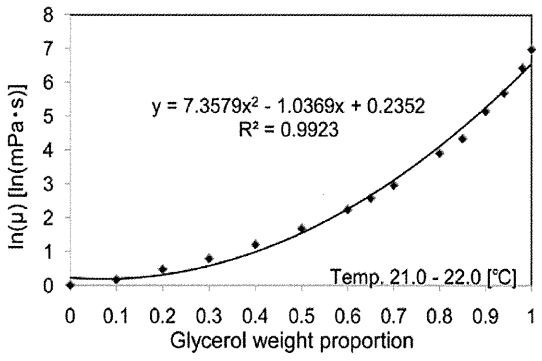

Fig. 4 Dynamic viscosity of natural logarithm of Gly. aq. and its fitted curve by quadratic polynomial as a function of glycerol weight proportion

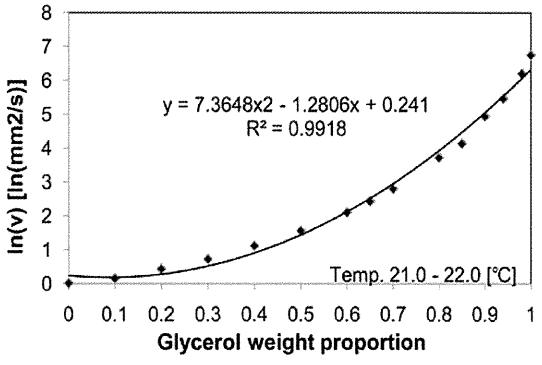

Fig. 5 Kinematic viscosity of natural logarithm of Gly. aq. calculated with measured values and its fitted curve by quadratic polynomial as a function of glycerol weight proportion

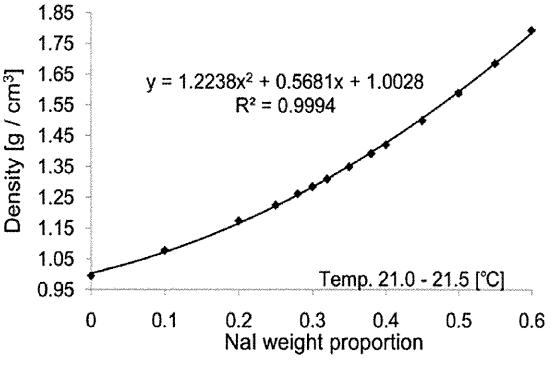

Fig. 6 Density of NaI. aq. and its fitted curve by quadratic polynomial as a function of NaI weight proportion

proposed, whereas, viscosities of NaI aq. exhibit external values and viscosities of NaI aq. are lower than those of blood with various concentrations. In conclusion, these results show that the adjustment method using a mixture can cover the kinematic viscosity of 3.8 mm^2/s used for BMF. The minimum and maximum refractive indices using Gly. aq. and NaI aq. with various kinematic viscosities are derived with the equations shown in the graphs of results.

The maximum range of the refractive index of the mixture over 3.8 mm^2/s is 1.472 when the 100 % glycerol was used for the mixture with NaI aq. In the case of a model with a refractive index higher than 1.472, combining liquids with higher refractive indices than the targeted value (*e.g.* [5] [17]) can be useful based on this adjustment method.

PIV measurements [15] or refractive index matching [16] with a combination of Gly. aq. and NaI aq. have been previously conducted. However, Sankovic et al. performed PIV only showing a mixture and Yusif et al. described a small amount of NaI used for adjustment of the refractive index to their model. Therefore, the use of a mixture for adjustment to a targeted refractive index and kinematic viscosity simultaneously is not yet optimized. In this research, we precisely investigated and examined data with respect to mixing, revealing that a direct decision about the mixing proportion of BMF is feasible. Even if refractive index needs to be adjusted and the kinematic viscosity needs to be changed for various experimental conditions, this mixing method is adaptable.

4.1. Viscosity of NaI aqueous solution

Our result has external values of viscosity of NaI at w = 0.3 - 0.4. That has not been described in previous studies [22, 23]. A capillary viscometer such as the ubbelohde-type viscometer was used in previous measurements. On the other hand, a vibration-type viscometer was used in present measurements. This difference of instrument may have affected the results. However, even if we found the external values of viscosity varying with NaI weight proportion, the tendency of viscosity changes can be the same as previous studies. When focusing on low viscosity, proper attention should be paid to the system of viscosity measurement.

4.2. Temperature dependency

The refractive index and viscosity of a material change as its temperature varies. Temperature dependence of the refractive index for a fluid was modeled with Eq. (7) as follows [17] [24].

$$n = a + bT \tag{7}$$

where a and b are constants and T is absolute temperature [K]. This constant b was empirically derived as b = −0.0002 for glycerol [17], and b = −0.000291 for NaI aq. [24] in previous papers. On the other hand, Yousif et al. estimated the effective refractive index at 1.4140 ±0.0008 with silicone model (Sylgard 184, Dow Corning). Based on their study, permissible deviation

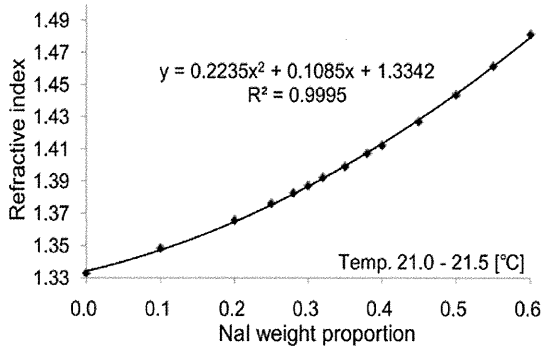

Fig. 7 Refractive index (to wavelength of fluorescent light) of NaI. aq. and its fitted curve by quadratic polynomial as a function of NaI weight proportion

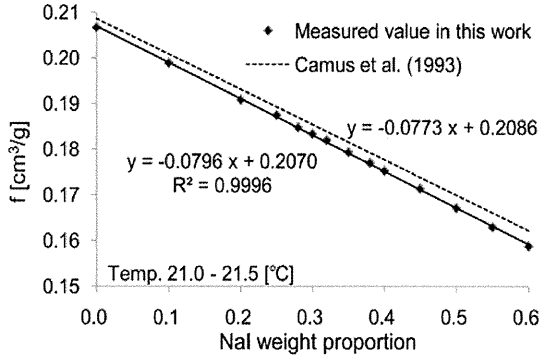

Fig. 8 Derived values of f with measured values of NaI aq. and its fitted curve by linearization as a function of NaI weight proportion compared with a previous report

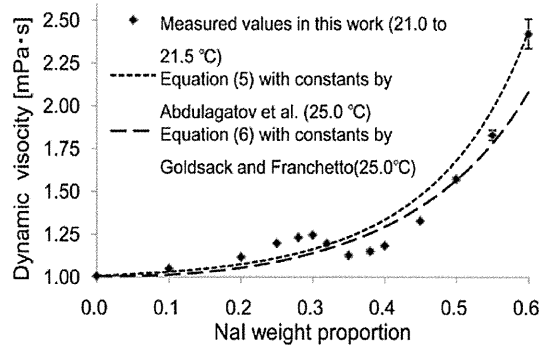

Fig. 9 Dynamic viscosity of NaI aq. as a function of NaI weight proportion compared with previous literatures